

COMPUTATIONAL ELECTROMAGNETICS OF METAL NANOPARTICLES AND THEIR AGGREGATES

The absorption and scattering of light by silver and gold nanoparticles and their aggregates provides a powerful mechanism for detecting important molecules in a variety of applications. Here, the authors describe recent advances in determining nanoparticle optical properties using computational electromagnetics.

Recently, there has been significant interest in using silver and gold nanoparticles as components of chemical and biological sensors. These particles are 1 to 100 nm in diameter, and we can prepare them using methods ranging from wet colloid chemistry to metal vapor deposition to lithographic masks. Artisans have used the colloidal particles since medieval times for stained glass windows (silver particles make yellow glass and gold particles provide red glass), but what is new to this field are two experimental capabilities. First is our ability to control particle structural properties (shape, size, local environment, and degree of aggregation) over a much larger range and with greater precision, so we can define optical properties (such as color) as needed. Second is our ability to functionalize the nanoparti-

cles (that is, chemically control what is on the particle surfaces) so that they will interact selectively with the molecules we want to detect.

Combining these two advances has produced new classes of chemical and biological sensors.^{1,2} These sensors have higher sensitivity and, in some cases, greater selectivity than conventional sensors for detecting a wide variety of molecules of importance in medical diagnostics, environmental remediation, identification of hazardous materials, and other applications. In addition, the small size of the sensor components (less than 100 nm) provides greater possibilities for developing multiplexed sensors that can simultaneously detect many molecules.

These new developments in nanotechnology provide opportunities for applying computational electromagnetics to determine and optimize nanoparticle optical properties. The nanoparticles of interest are typically large enough that classical electromagnetic theory can accurately describe their interaction with light but small enough so that there are strong variations in optical properties with particle size,

1521-9615/01/\$10.00 © 2001 IEEE

K. LANCE KELLY, ANNE A. LAZARIDES, AND GEORGE C. SCHATZ
Northwestern University

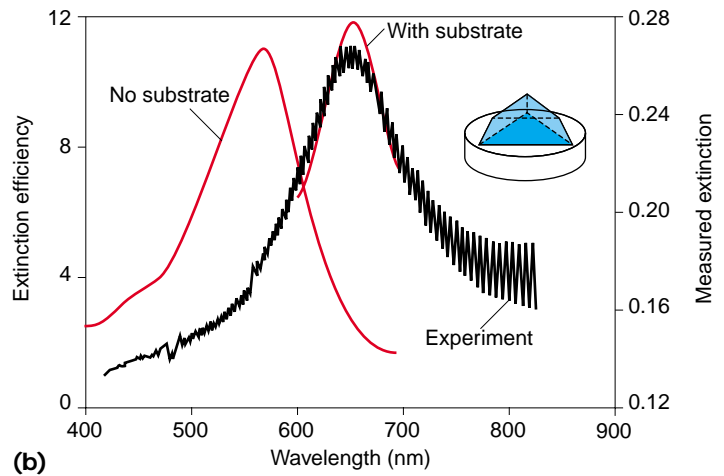
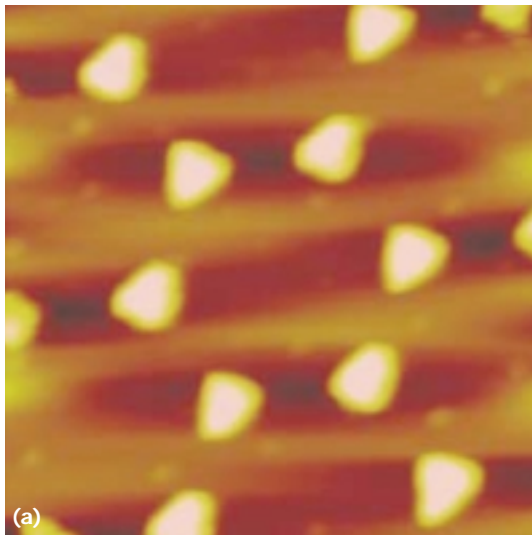


Figure 1. (a) Atomic force microscope images of lithographically prepared particles; (b) measured spectra associated with these particles, along with the results from discrete-dipole-approximation calculations.

shape, and local environment. These many variables have positioned theory and computation to play a vital role in optimizing sensor design. However, because of the complexity of the systems being studied (metal nanoparticles, coated with one or more layers of molecules, and often located on a substrate with other nanoparticles nearby), efficient computational methods capable of treating complex materials are essential.

Nanoparticle-based sensors

Figure 1 shows one example of nanoparticles being developed for chemical sensor applications.¹ Figure 1a shows triangle-shaped silver particles that are prepared by vapor deposition through a colloidal crystal mask using a technique known as *nanosphere lithography*. This mask is prepared using commercially available polystyrene spheres, and because the spheres come in a wide variety of sizes, it is possible to make the particles with footprints ranging from 10 nm to microns. In addition, by controlling the vapor deposition, the heights of the particles can vary over a wide range. This combination of footprint and height control lets us vary the wavelength of maximum absorption (the so-called plasmon resonance wavelength) throughout the spectrum's visible and near-infrared regions. In addition, the plasmon wavelength is sensitive to the presence of molecules absorbed on the nanoparticle surface; this sensitivity lets us use the particles as chemical sensors. Figure 1b shows a plasmon resonance absorption spectrum, along with a computational result that we will describe later.

Figure 2 shows a second example of a nanoparticle-based sensor. Here we show an image of 13-nm colloidal gold nanoparticles that have been aggregated with DNA to link the particles.² To do this, we first attach single-stranded oligonucleotides to the gold particles and then induce aggregation by adding complementary oligonucleotides that link the particles together

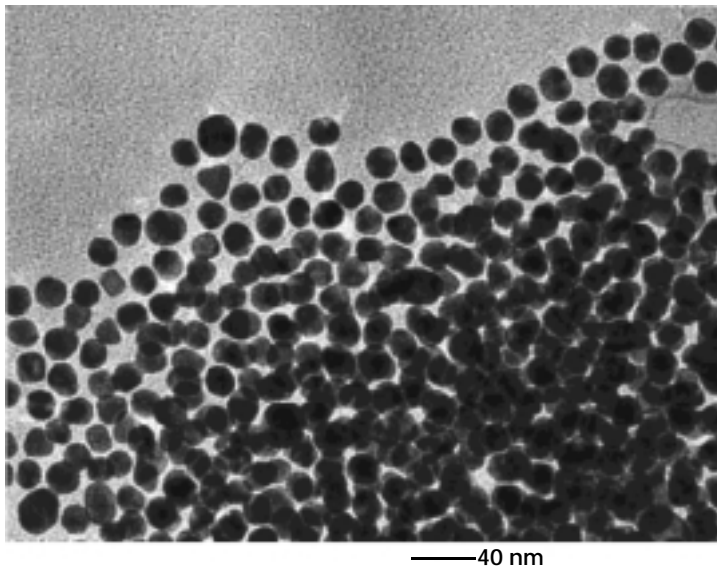


Figure 2. Scanning electron microscope images of DNA-linked gold particle aggregates. The particle diameter is 13 nm, and the DNA linkers are 72 base-pair duplexes.

upon hybridization. This aggregation process produces a color change in the gold nanoparticles from red to blue (due to a complimentary shift in the plasmon wavelength from 520 nm to 580 nm), because the DNA-linked particles are close enough together in the aggregates that they exhibit electromagnetic coupling. As a result, we can use the color of the aggregates as a sensor for the presence of the DNA link. This color change depends on a variety of factors (such as the particle size and the DNA length), and under optimum conditions, it is possible to detect a few thousand molecules of DNA.

Light absorption and scattering by nanoparticles

The classical electromagnetic theory of metal nanoparticles has a long history, going back nearly a century to Mie's celebrated solution to Maxwell's equations for the scattering of light by a spherical particle.³ (We present one form of Maxwell's equations in the sidebar). Mie's theory is limited to spherical particles, but we can use it to describe particles of any size, provided that the particles are large enough so that classical electromagnetic theory applies (down to about 1 nm, provided we use size-dependent dielectric constants). Computationally speaking, for sphere sizes approaching visible wavelengths, the calculations become increasingly intensive. However, even for optically dense materials such as metals, modern codes are so efficient that even a personal computer is adequate for Mie theory.

For asymmetric nanoparticles—or even spherical nanoparticles in an asymmetric environment—we turn to numerical methods for solving Maxwell's equations. Researchers have developed several numerical methods in the last few years, usually motivated by interests in other fields—such as light scattering by biomolecules, grains in the interstellar medium, and macroscopic objects. The numerically exact methods used to describe nonspherical metal nanoparticles including

- discrete dipole approximation (DDA),^{4,5}
- multiple multipole methods (MMP),⁶
- finite difference time domain (FDTD) methods,⁷ and
- T-matrix methods.⁸

DDA methods divide the particle into numerous polarizable cubes. The induced dipole polarizations in these cubes are determined self-consistently, then properties such as the ex-

inction cross section are determined in terms of the induced polarizations (see the sidebar). The time-consuming part of the calculation involves evaluating dipole fields at each cube due to polarization in the other cubes. We

Maxwell's Equations: Discrete Dipole Approximation

Maxwell's equations describe fields in the presence of matter:

$$\nabla \cdot \mathbf{D} = \rho_f \quad \text{Gauss's law}$$

$$\nabla \cdot \mathbf{B} = 0$$

$$\nabla \times \mathbf{E} = -\partial \mathbf{B} / \partial t \quad \text{Faraday's law}$$

$$\nabla \times \mathbf{H} = \mathbf{J}_f + \partial \mathbf{D} / \partial t \quad \text{Ampère's law with Maxwell's correction}$$

where \mathbf{E} and \mathbf{H} are the electric and magnetic fields, \mathbf{D} is the electric displacement, \mathbf{B} is the magnetic induction, ρ_f is the charge density, and \mathbf{J}_f is the current density.

We can calculate an approximate solution to Maxwell's equations for a body of any shape in a given incident field, \mathbf{E}_{inc} , using a discrete representation of the shape. For a nonmagnetic material in a plane wave field, we can approximate the response with a cubic lattice of interacting electric dipoles, each with a polarization

$$\mathbf{P}_i = \alpha_i \cdot \mathbf{E}_{loc,i}$$

where α_i is each dipole's polarizability. The local field at each dipole is given by

$$\begin{aligned} \mathbf{E}_{loc,i} &= \mathbf{E}_{inc,i} + \mathbf{E}_{dip,i} \\ &= \mathbf{E}_0 \exp(i \mathbf{k} \cdot \mathbf{r}_i) - \sum_{j \neq i} \mathbf{A}_{ij} \cdot \mathbf{P}_j \end{aligned}$$

and the interaction matrix is

$$\begin{aligned} \mathbf{A}_{ij} \cdot \mathbf{P}_j &= \frac{\exp(ikr_{ij})}{r_{ij}^3} \cdot \\ &\left\{ k^2 \mathbf{r}_{ij} \times (\mathbf{r}_{ij} \times \mathbf{P}_j) + \frac{(1 - ikr_{ij})}{r_{ij}^2} [\mathbf{r}_{ij}^2 \mathbf{P}_j - 3\mathbf{r}_{ij}(\mathbf{r}_{ij} \cdot \mathbf{P}_j)] \right\}_{(j \neq i)} \end{aligned}$$

where $k = \omega/c$, $r_{ij} = |\mathbf{r}_i - \mathbf{r}_j|$, and $\mathbf{r}_{ij} = \mathbf{r}_i - \mathbf{r}_j$. Once we find the polarizations \mathbf{P}_j , the extinction and absorption cross sections C_{ext} and C_{abs} are

$$\begin{aligned} C_{ext} &= \frac{4\pi k}{|\mathbf{E}_0|^2} \sum_{i=1}^N \text{Im}(\mathbf{E}_{inc,i}^* \cdot \mathbf{P}_i) \\ C_{abs} &= \frac{4\pi k}{|\mathbf{E}_0|^2} \sum_{i=1}^N \left\{ \text{Im}[\mathbf{P}_i \cdot (\alpha_i^{-1})^* \mathbf{P}_i] - \frac{1}{3} k^3 |\mathbf{P}_i|^2 \right\} \end{aligned}$$

For a material with complex refractive index m , DDA is valid when $|m|kd \ll 1$. Computational requirements of DDA are roughly proportional to $N \log(N)$, where N is the calculation's total number of dipoles.

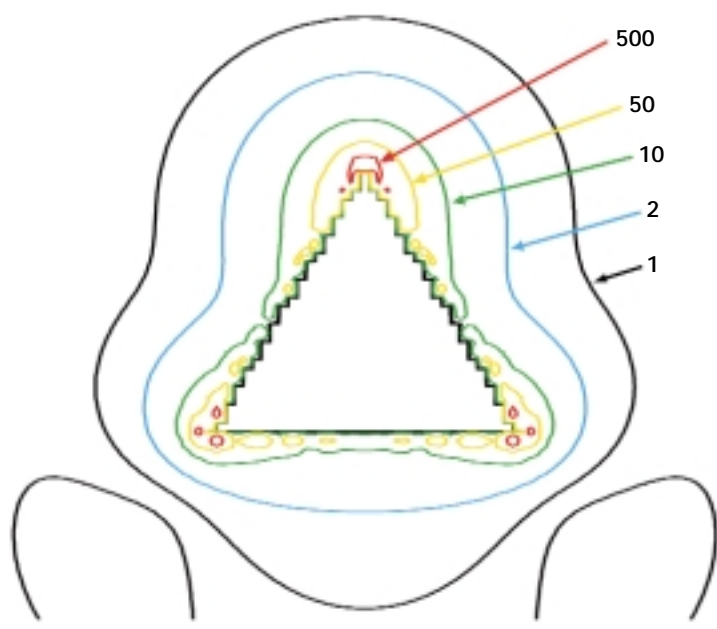


Figure 3. Electric fields (plotted as contours of $|E|^2$) around the surface of a lithographically prepared, triangular particle.

can evaluate these fields using Fourier methods, leading to an $N \log(N)$ dependence of computation time on the number of cubes.

The MMP method divides the particle into domains with shapes that allow for series expansion solutions of Maxwell's equations. We can then determine the coefficients in these expansions by matching boundary conditions at the domain interfaces. We match the boundary conditions using least-squares so that the resulting solution is exact within each domain but approximate at the boundaries. In this case, the computational effort varies with the number of matching points, expansion functions, and basis functions used in the expansions.

FDTD methods solve Maxwell's equations as a function of time (rather than at a fixed frequency as with the other methods) using a 3D Cartesian grid for expressing the spatial derivatives. There is also a finite-element version of the same theory.

T-matrix methods express the fields inside and outside the object as expansions in vector spherical harmonics. We can determine the coefficients in this expansion by matching boundary conditions at the particle surfaces. Instead of least squares matching, as in the MMP calculation, the solutions are exactly matched within the subspace of the spherical harmonic basis by projecting the matching equations onto the basis functions.

Figure 1b presents results of applying the DDA method to determine the extinction spectrum of a triangular nanoparticle similar to those presented in Figure 1a. Two results are presented—one where no substrate is present (that is, the particle is suspended in a vacuum) and one explicitly defining a slab of substrate material beneath the particle. Here, the quantity plotted versus wavelength is the extinction efficiency, which is the absorption cross section plus the scattering cross section normalized by the physical cross section. The triangular nanoparticles of silver are constructed as truncated tetrahedrons, and, for the case when a mica substrate is included, the tetrahedron sits on a cylindrical disk (see the inset in Figure 1b). In this case, the agreement between the resonance wavelength of theory and experiment occurs only when the substrate slab is included. The agreement including the slab is good, indicating that approximations made in modeling the particle structure—and in the assumed dielectric constants—are not severe. In addition, the particles are spaced far enough away from each other that interparticle electromagnetic coupling is weak. Thus, only the environment immediately adjacent to the particles is important.

Figure 3 shows the fields immediately adjacent to a triangular nanoparticle, such as that pictured in Figure 1b, for a linearly polarized incident beam at the resonance wavelength (polarization is along the perpendicular bisector). The nanoparticle's depicted cross section corresponds to the base (note that the substrate was not included for this calculation). As expected, the contours indicate that the electric field is enhanced at the particle tips, which suggests that these locations on the particle are much more sensitive to nearby molecules than are spherical nanoparticles. Also apparent in the contours are singularities in the field near the exposed cubes. This is an unfortunate drawback of the DDA method for determining precise information about fields near the particle surfaces and is a subject of current research.

Light absorption and scattering by nanoparticle aggregates

Different challenges arise when the coupling between nanoparticles drives the phenomenon of interest, such as the aggregates in Figure 2. Rigorous description of the optical response of such systems requires investigating the effect of particle size, interparticle spacing, and overall

aggregate shape and size. Fortunately, experimental constraints limit many of these parameters, and we can greatly decrease the computational effort in many circumstances.

Full electrodynamic treatment of interacting spherical particles requires that each particle be described by an expansion of many spherical harmonics, as Mie theory describes for a single sphere. When many spheres are present, such as in the aggregates found experimentally, the coupled multipole system describes a computationally rigorous approach to determining extinction and scattering spectra.⁹ However, the computational effort associated with this approach scales as a high power of the maximum order multipole included in the calculation, so the computational effort can be substantial.

Using coupled multipoles, we have previously shown that, for small colloidal gold particles separated by distances of a radius or more, only the first (dipole) term of the expansion is necessary for an accurate description of the optical response.¹⁰ Therefore, we can simplify the problem to *coupled dipoles*. In addition, if the particles are assumed to be located on a cubic lattice, then we can efficiently evaluate the dipole sums using Fourier methods, thereby including a much larger number of particles (up to 10^5).¹¹ Such a CD calculation is computationally identical to a DDA calculation; however, don't mistake the method of CDs for DDA. The dipole lattice in DDA is designed to describe a homogeneous material, whereas in CD, the dipoles represent spherical nanoparticles surrounded by a medium that is composed of water and adsorbed molecules (such as DNA). The lattice in CD calculations need not be completely populated—indeed, random occupation is useful for simulating some types of aggregates.

Figure 4 represents a spherical aggregate of CDs in a body-centered cubic array. The two colors represent the two different oligonucleotide labels required in the experiment. Figure 5 shows that for aggregates similar to those pictured in Figure 2, the CD approach reproduces the answer obtained using the more expensive coupled multipole calculation. Figure 6a illustrates experimental extinction spectra of dispersed gold nanoparticles and DNA-linked nanoparticle aggregates.^{2,11} Figure 6b shows the CD predictions of extinction spectra for a range of aggregate sizes,¹¹ all for spherically shaped aggregates consisting of 13-nm gold particles on a body-centered cubic lattice with nearest neighbor separations of 6.5 nm. The extinction spec-

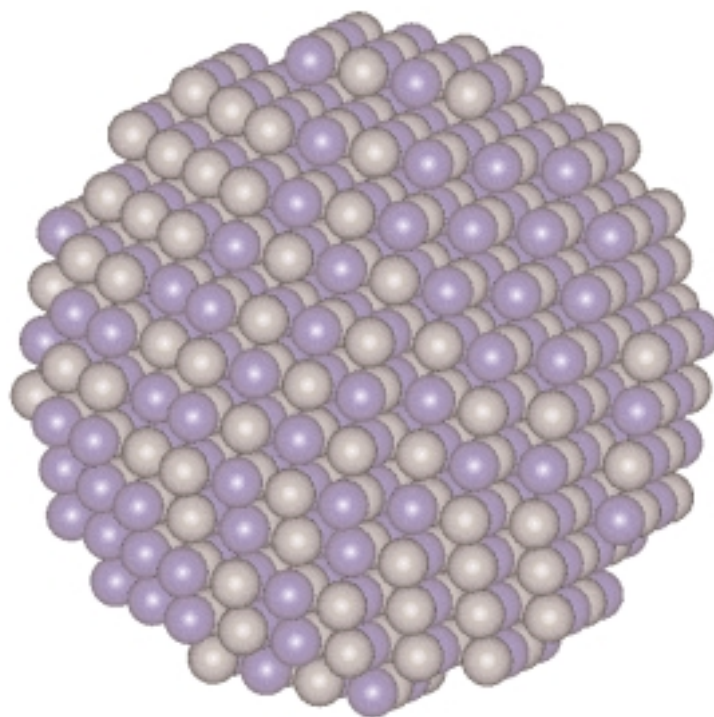


Figure 4. The structural model used to describe nanoparticle aggregates based on gold particles with DNA links. The two colors represent gold particles having two noncomplementary oligonucleotides attached. The DNA link in this case will only bind particles with different oligonucleotides to each other, therefore yielding the indicated binary aggregates.

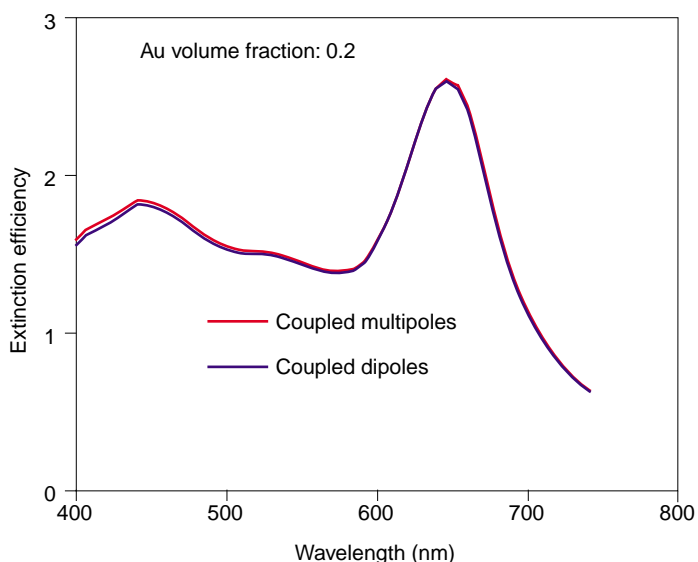


Figure 5. A comparison of coupled dipole and coupled multipole calculations of extinction for a spherical aggregate of 89 30-nm gold nanospheres in an aqueous medium. The particles are arranged in a body-centered cubic array with 15 nm between neighbors.

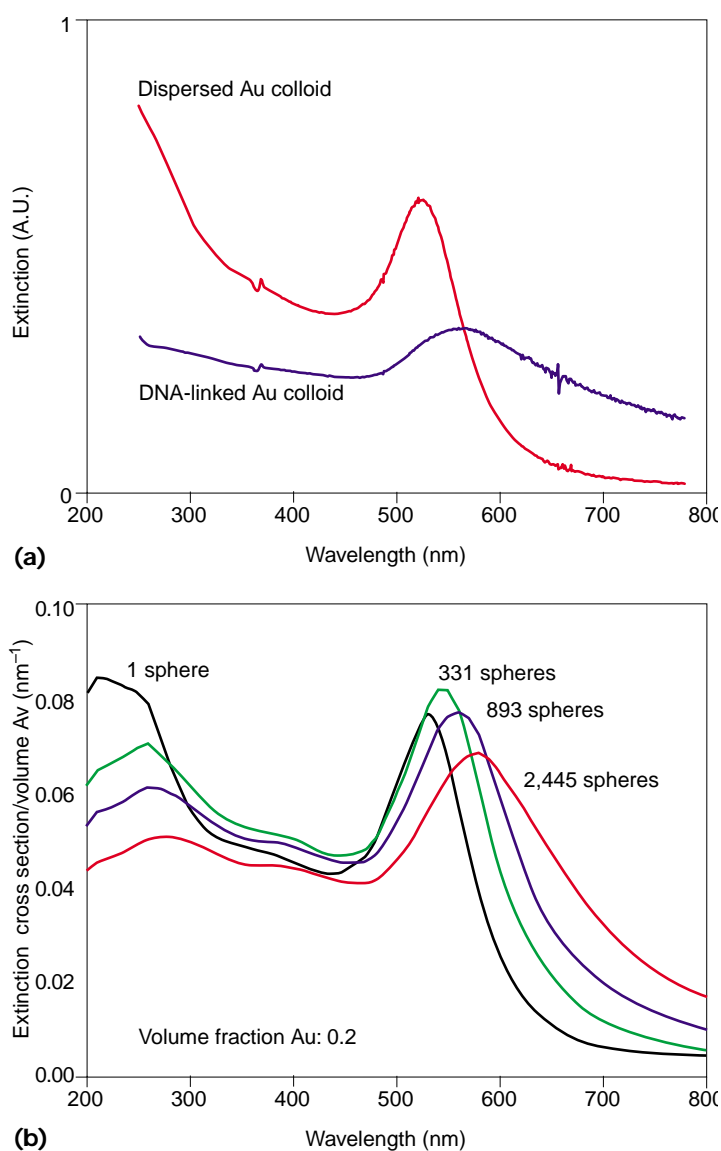


Figure 6. Extinction spectra for dispersed and DNA-linked gold nanoparticles: (a) The 13-nm particles are capped with 3'- and 5'-(alkanethiol) 12-base oligonucleotides. Complementary 24-base oligonucleotide links particles capped with the 3'-(alkanethiol) 12-base oligo to particles capped with the 5'-(alkanethiol) 12-base oligo. (Experimental data courtesy of James J. Storhoff, Robert C. Mucic, Chad A. Mirkin, and Robert L. Letsinger.) (b) Spectra calculated for dispersed (the Mie theory) and linked (coupled dipoles) gold nanoparticles.


trum calculated for the largest aggregate matches approximately the experimental data for linked particles. In other calculations, we have demonstrated that these spectra are not significantly dependent on aggregate shape¹² and have

quantified the effect of disorder within the aggregate.¹⁰ Thus, the comparisons we present between theory and experiment are realistic.

We can reduce computational requirements even more substantially for this system if we model the nanoparticle aggregate (and media contained therein) as a homogenous material or effective medium.¹² This can be done in the context of the Maxwell-Garnett theory (an electrostatic approach) or using an electrodynamic effective medium theory. The latter involves inverting the lattice-dispersion relation—the same relation used to find the polarizabilities of each dipole of the DDA method described earlier—to determine the dielectric function as a function of wavelength for the aggregate material. With this dielectric function, we can describe the extinction of a spherical aggregate using the Mie theory, which, as we mentioned, has negligible computational cost. In addition, we can use the aggregate material dielectric function in any numerical implementation of the Maxwell theory, such as the DDA method, to describe nonspherical aggregates. DDA calculations for aggregates comparable to those considered in Figure 6b yield results essentially identical to those in Figure 6.¹² Of course, the CD or coupled multipole theories are more powerful and allow for the study of aggregates where effective medium theory breaks down (large particles, disordered aggregates).

The primary goal of the research we present here has been to use computational electrodynamic methods to calculate the spectra of gold and silver nanoparticles and aggregates of nanoparticles. We demonstrated that available finite-element and coupled multipole and dipole methods can describe such spectra quantitatively. This means that we can now use these methods with confidence to predict spectra of nanoparticle systems that have not yet been made and, moreover, to determine what kinds of systems are the most interesting for chemical and biological sensing applications.

Although the computational methods demonstrated here are adequate for determining spectra for the problems we have considered so far, there are many limitations in the present genera-

tion of methods that will require further research in the development of improved methods. For example, the DDA approach is very good for determining extinction spectra, but it has severe limitations in determining the electromagnetic fields around the particles, as Figure 3 shows. Determining fields will let us tackle the interesting question of optimized nanoparticle configurations for doing single molecule spectroscopy and for describing surface-enhanced Raman intensities. Other methods, such as the MMP approach, provide more powerful capabilities for determining electromagnetic fields, but applying these to the nanoparticle systems described here has not yet been demonstrated. 

Acknowledgment

This research was supported by ARO Grant DAAG55-97-1-0133 and by the NSF's MRSEC program (Grant DMR-0076097).

References

1. M.D. Malinsky et al., "Nanosphere Lithography: Effect of the Substrate on the Localized Surface Plasmon Resonance Spectrum of Silver Nanoparticles," *J. American Chemical Society*, vol. 123, no. 12, Mar. 2001, pp. 1471–1482.
2. J.J. Storhoff et al., "What Controls the Optical Properties of DNA-Linked Gold Nanoparticle Assemblies?" *J. American Chemical Society*, vol. 122, no. 19, May 2000, pp. 4640–4650.
3. C.F. Bohren and D.R. Huffman, *Absorption and Scattering of Light by Small Particles*, Wiley Interscience, New York, 1983.
4. T. Jensen et al., "Electrodynamics of Noble Metal Nanoparticles and Nanoparticle Clusters," *J. Cluster Science*, vol. 10, no. 4, Apr. 1999, pp. 295–317.
5. B.T. Draine and P.J. Flatau, "Discrete-Dipole Approximation for Scattering Calculations," *J. Optical Society of America A*, vol. 11, no. 4, Apr. 1994, pp. 1491–1499.
6. L. Novotny, D.W. Pohl, and B. Hecht, "Scanning Near-Field Optical Probe with Ultrasmall Spot Size," *Optical Letters*, vol. 20, no. 9, May 1995, pp. 970–972.
7. A. Taflov, *Computational Electrodynamics: The Finite-Difference Time-Domain Method*, Artech House, Boston, 1995, p. 599.
8. P.W. Barber and S.C. Hill, *Light Scattering by Particles: Computational Methods*, World Scientific, Singapore, 1990.
9. D.W. Mackowski and M.I. Mishenko, "Calculation of the T Matrix and the Scattering Matrix for Ensembles of Spheres," *J. Optical Society America A*, vol. 35, no. 11, Nov. 1996, pp. 2266–2278.

10. A.A. Lazarides and G.C. Schatz, "DNA-Linked Metal Nanosphere Materials: FFT Solution for the Optical Response," *J. Chemical Physics*, vol. 112, no. 6, Feb. 2000, pp. 2987–2993.
11. A.A. Lazarides and G.C. Schatz, "DNA-Linked Metal Nanosphere Materials: Structural Basis for the Optical Properties," *J. Physical Chemistry B*, vol. 104, no. 3, Jan. 2000, pp. 460–467.
12. A.A. Lazarides, K.L. Kelly, and G.C. Schatz, "Effective Medium Theory of DNA-Linked Gold Nanoparticle Aggregates: Effect of Aggregate Shape," to be published in *Proc. Materials Research Society Meeting*, vol. 635, 2001.

K. Lance Kelly is a PhD candidate in the Department of Chemistry at Northwestern University. His research at Northwestern deals with the electrodynamics of noble metal nanoparticles and nanoparticle aggregates. He received his BS from Texas A&M University. Contact him at the Dept. of Chemistry, Northwestern Univ., Evanston, IL 60208-3113; akite@chem.nwu.edu.

Anne A. Lazarides is a research assistant professor at Northwestern University. Currently, she is associated with Prof. Chad Mirkin's research program, where she leads the effort in structural characterization of hybrid bioinorganic nanoparticle materials. Her interests include nanoparticle materials theory, particularly nanomaterial optical properties. She received her PhD from Princeton University and did postdoctoral work at Xerox and at Northwestern University. Contact her at the Dept. of Chemistry, Northwestern Univ., Evanston, IL 60208-3113; lazarides@northwestern.edu.

George C. Schatz is a professor of chemistry at Northwestern University. His research focuses on materials theory, especially the optical properties of surfaces, nanoparticles, and nanoparticle aggregates. He also works with oligonucleotide structural modeling, reaction dynamics, scattering theory, molecular dynamics, and potential energy surfaces. He received his PhD from Caltech and was a postdoctoral fellow at MIT before moving to Northwestern. Contact him at the Dept. of Chemistry, Northwestern Univ., Evanston, IL 60208-3113; schatz@chem.nwu.edu.